Squeezing and Einstein-Podolsky-Rosen correlation in the mirrorless optical parametric oscillator

A. Gatti,[1,2,*] T. Corti,[1] and E. Brambilla[1]

[1]*Istituto di Fotonica e Nanotecnologie del CNR, Piazza Leonardo da Vinci 32, Milano, Italy*

[2]*Dipartimento di Scienza e Alta Tecnologia dell'Università dell'Insubria, Via Valleggio 11 Como, Italy*

(Received 6 March 2017; published 11 July 2017)

This work analyses the quantum properties of counterpropagating twin beams generated by a mirrorless optical parametric oscillator in the continuous-variable regime. Despite the lack of the filtering effect of a cavity, we show that in the vicinity of its threshold it may generate high levels of narrowband squeezing and Einstein-Podolsky-Rosen correlation, completely comparable to what can be obtained in standard optical parametric oscillators.

DOI: 10.1103/PhysRevA.96.013820

Backward parametric down-conversion (PDC), where one of the twin beams back-propagates with respect to the pump laser source (Fig. 1), is gaining increasing attention in the quantum optics community. In the spontaneous regime it has a natural potential to generate high-purity and narrowband heralded single photons [1–3], a highly desirable and nontrivial goal, which in the standard copropagating geometry can be realized only at specific tuning points.

A second appealing feature is the presence of a threshold pump intensity, beyond which the system makes a transition to coherent oscillations; i.e., it behaves as a *mirrorless optical parametric oscillator* (MOPO) [4]. Responsible for this critical behavior is the feedback mechanism established by back-propagation and stimulated down-conversion. Corti *et al.* [5] analyzed the critical behavior of twin beams below threshold, enlightening the role of the quantum correlation of photon pairs in creating the feedback necessary to the onset of a classical coherence above threshold.

In this work we turn our attention to the quantum properties of the source in the continuous-variable regime, so far unexplored, namely, its potentiality to generate Einstein-Podolsky-Rozen (EPR)-correlated beams in the vicinity of the threshold. EPR correlations [6–8], i.e., nonclassical correlations in a pair of noncommuting field quadratures, and their associated squeezing, are features of the two-mode squeezed state produced by any down-conversion process (see, e.g., Ref. [9]). However, squeezed light generated in the standard single-pass configuration is in general multimode, which is often undesirable for applications [10] Moreover high levels of squeezing are hard to generate and detect (see, e.g., Ref. [11], but also Refs. [12,13] for recent achievements in this sense). The typical solution is to recycle the parametric light in an optical resonator, which at the same time enforces the nonlinearity and produces a sharp modal filtering, i.e., to build an optical parametric oscillator (OPO). Remarkably, this work will show that counterpropagating twin beams, despite the lack of the filtering effect of the cavity, exhibit high levels of narrowband EPR correlation, completely comparable to what can be obtained in standard subthreshold OPOs. The role of the cavity in the MOPO is played by the distributed feedback mechanism [5], which creates a threshold where, similarly to the OPO, the quantum noise in principle diverges in some observables, allowing then noise suppression in their conjugate observables. Once technical challenges involved in its realization are overcome, this source may then represent a robust and compact alternative to the OPO.

The backward geometry requires a submicrometer poling of the $\chi^{(2)}$ materials, which explains why after the first theoretical prediction [14], this source had to wait 40 yr before being realized [4]. We consider the scheme in Fig. 1, in which the laser pump at frequency ω_p and the signal at frequency ω_s copropagate along the $+z$ axis in the nonlinear medium, while the idler at frequency $\omega_i = \omega_p - \omega_s$ back-propagates in the $-z$ direction. Quasi-phase matching (i.e., the generalized momentum conservation) is realized when their corresponding wave numbers $k_j = \omega_j n_j(\omega_j)/c$ satisfy

$$k_s - k_i = k_p - m\frac{2\pi}{\Lambda}, \qquad m = 1,3,\ldots, \tag{1}$$

where Λ is the poling period and n_j are the refraction indexes. First-order interactions then require $\Lambda \simeq \lambda_p/n_p$.

Our quantum model for this configuration is described in Refs. [2,5] (see also Ref. [15]). As in the former literature, we restrict to a purely temporal description, assuming either waveguiding or a small collection angle. Below the MOPO threshold the depletion of the pump laser is negligible, and it can be described as a classical field of constant amplitude along the sample. Assuming in addition the pump field is a continuous wave, it is simply described by its complex amplitude $\alpha_p = |\alpha_p|e^{i\phi_p}$. The strength of the parametric interaction is then characterized by the dimensionless gain

$$g = \sqrt{2\pi}\,\chi\,|\alpha_p|l_c, \tag{2}$$

where χ is proportional to the $\chi^{(2)}$ susceptibility of the medium and l_c is the crystal length. In terms of this parameter the MOPO threshold occurs [16] at

$$g = g_{\rm thr} = \frac{\pi}{2}. \tag{3}$$

The signal and idler waves are instead described by the quantum field operators $\hat{A}_s(\Omega,z)$ and $\hat{A}_i(\Omega,z)$, for two wave-packets centered around the respective reference frequencies ω_s and ω_i satisfying quasi-phase matching (1) (capital Ω is the offset from the ω_j). As detailed in Ref. [5], the model is

*Corresponding author: Alessandra.Gatti@mi.infn.it

 ©2017 American Physical Society

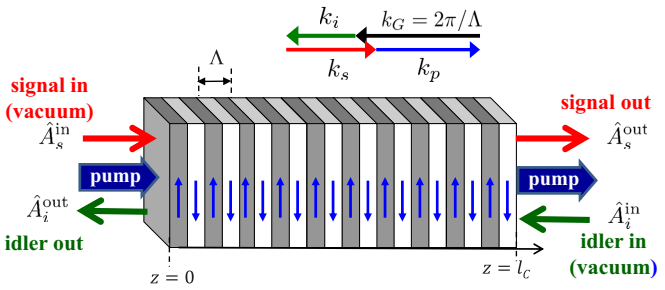

FIG. 1. Scheme of backward PDC, taking place in a $\chi^{(2)}$ crystal periodically poled with a submicrometer period $\Lambda \approx \lambda_p/n_p$. Quasi-phase matching [Eq. (1)] requires then that the idler field is generated in the backward direction with respect to the signal and the pump.

formulated in terms of linear propagation equations coupling only the frequency conjugate modes $\omega_s + \Omega$ and $\omega_i - \Omega$ of the twin beams, whose solution gives a transformation linking the output operators $\hat{A}_s^{\rm out} = \hat{A}_s(z = l_c)$ and $\hat{A}_i^{\rm out} = \hat{A}_i(z = 0)$ to the input ones (Fig. 1), assumed in the vacuum state. Notice that in this geometry the boundary conditions are not the standard ones, because the signal and idler fields exit from the opposite end faces of the slab. The input-ouput relations are then the Bogoliubov transformation, characteristic of processes where particles are generated in pairs:

$$\hat{A}_s^{\rm out}(\Omega) = U_s(\Omega)\hat{A}_s^{\rm in}(\Omega) + V_s(\Omega)\hat{A}_i^{\rm in\dagger}(-\Omega), \tag{4a}$$

$$\hat{A}_i^{\rm out}(-\Omega) = U_i(-\Omega)\hat{A}_i^{\rm in}(-\Omega) + V_i(-\Omega)\hat{A}_s^{\rm in\dagger}(\Omega). \tag{4b}$$

The coefficients $U_j(\Omega)$ and $V_j(\Omega)$ are the trigonometric functions [5]:

$$U_s(\Omega) = e^{ik_s l_c} e^{i\beta(\Omega)} \phi(\Omega), \tag{5a}$$

$$V_s(\Omega) = e^{i(k_s - k_i)l_c} g e^{i\phi_p} \frac{\sin\gamma(\Omega)}{\gamma(\Omega)} \phi(\Omega), \tag{5b}$$

$$U_i(-\Omega) = e^{ik_i l_c} e^{i\beta(\Omega)} \phi^*(\Omega), \tag{5c}$$

$$V_i(-\Omega) = g e^{i\phi_p} \frac{\sin\gamma(\Omega)}{\gamma(\Omega)} \phi^*(\Omega), \tag{5d}$$

with

$$\phi(\Omega) = \frac{1}{\cos\gamma(\Omega) - i\frac{\mathcal{D}(\Omega) l_c}{2\gamma(\Omega)} \sin\gamma(\Omega)}, \tag{5e}$$

$$\gamma(\Omega) = \sqrt{g^2 + \frac{\mathcal{D}^2(\Omega) l_c^2}{4}}. \tag{5f}$$

In these expressions,

$$\mathcal{D}(\Omega) = k_s(\Omega) - k_i(-\Omega) - k_p + k_G \tag{6}$$

is the phase mismatch for two frequency conjugate signal-idler components, $k_j(\Omega)$ being the wave number of the jth wave at frequency $\omega_j + \Omega$ ($j = s,i$). The phase

$$\beta(\Omega) = [k_s(\Omega) + k_i(-\Omega) - (k_s + k_i)]\frac{l_c}{2} \tag{7}$$

is a global propagation phase. Notice that the coefficients $U_j(\Omega)$ and $V_j(\Omega)$ diverge when approaching the MOPO threshold $g = \pi/2$, and, as can be easily checked, they satisfy the unitarity conditions: $|U_j(\Omega)|^2 - |V_j(\Omega)|^2 = 1$ and $U_s(\Omega)V_i(-\Omega) = U_i(-\Omega)V_s(\Omega)$.

Unlike the copropagating case, this configuration is characterized by narrow spectral bandwidths [2,4,5]. Therefore, it is legitimate to retain only the first order of the Taylor expansions of the wave numbers $k_j(\Omega)$, so that

$$\frac{\mathcal{D}(\Omega) l_c}{2} \simeq \frac{l_c}{2}(k_s' + k_i')\Omega = \frac{\Omega}{\Omega_{\rm gvs}}, \tag{8}$$

$$\beta(\Omega) \simeq (k_s' - k_i')\frac{l_c}{2}\Omega = \frac{\Omega}{\Omega_{\rm gvm}}, \tag{9}$$

where $k_j' = \frac{dk_j}{d\Omega}|_{\Omega=0}$, and

$$\Omega_{\rm gvs}^{-1} \equiv \tau_{\rm gvs} = \frac{1}{2}\left[\frac{l_c}{v_{gs}} + \frac{l_c}{v_{gi}}\right] \tag{10}$$

is a *long* time scale characteristic of counterpropagating interactions, on the order of the transit time of light along the slab, involving the *sum* of the inverse group velocities $v_{gj} = 1/k_j'$ [2,5]. In the spontaneous regime, it defines the correlation time of twin photons, while its inverse $\Omega_{\rm gvs}$ gives the narrow width of their spectrum, which becomes even narrower in the stimulated regime and ideally shrinks to zero on approaching threshold [5]. Conversely

$$\Omega_{\rm gvm}^{-1} \equiv \tau_{\rm gvm} = \frac{l_c}{2v_{gs}} - \frac{l_c}{2v_{gi}} \tag{11}$$

is a *short* time scale related to the group velocity mismatch (GVM) and produces a small temporal offset between the signal and idler wave-packets. Clearly, $|\Omega_{\rm gvm}| \gg \Omega_{\rm gvs}$ for any tuning conditions (see Fig. 5 for a comparison in the case of $LiNbO_3$). Within these linear approximations the coefficients $U_j(\Omega)$ and $V_j(\Omega)$ basically depend on the frequency only through the ratio $\frac{\Omega^2}{\Omega_{\rm gvs}^2}$, because $\gamma(\Omega) \simeq \sqrt{g^2 + \frac{\Omega^2}{\Omega_{\rm gvs}^2}}$, while the phase $\beta(\Omega)$ in Eq. (9) varies on the slow scale $|\Omega_{\rm gvm}| \gg \Omega_{\rm gvs}$ and remains close to zero in the spectral region where $U_j(\Omega)$ and $V_j(\Omega)$ take nontrivial values.

Several properties of the state of the MOPO below threshold depend solely on the Bogoliubov form (4) of the transformation, so that they are common to any linear process of photon-pair generation. In particular, if one introduces the sum and difference between frequency conjugate components of the twin beams, $\hat{C}_\pm(\Omega) = \frac{1}{\sqrt{2}}[\hat{A}_s^{\rm out}(\Omega) \pm A_i^{\rm out}(-\Omega)]$, then the transformation (4) decouples into two independent *squeeze* transformations [17]. The $\pm$ modes are thus individually squeezed, and their squeezing ellipses turn out oriented along orthogonal directions. As is well known, this implies the simultaneous presence of correlation and anticorrelation in two orthogonal quadrature operators of the twin beams [7,8].

In order to characterize the amount of squeezing and EPR correlation generated in this specific configuration, let us consider the quadrature operators for the individual signal and idler fields in the time domain:

$$\hat{X}_j(t) = \hat{A}_j^{\rm out}(t)e^{-i\phi_j} + \hat{A}_j^{\rm out\,\dagger}(t)e^{i\phi_j}, \tag{12}$$

$$\hat{Y}_j(t) = \frac{1}{i}\left[\hat{A}_j^{\rm out}(t)e^{-i\phi_j} - \hat{A}_j^{\rm out\,\dagger}(t)e^{i\phi_j}\right] \quad j = s,i. \tag{13}$$

The two orthogonal quadratures do not commute $[\hat{X}_j(t), \hat{Y}_k(t')] = \delta_{j,k}\delta(t-t')$ and represent incompatible observables. Notice that their Fourier transforms, $\hat{X}_j(\Omega) = \hat{A}_j^{\text{out}}(\Omega)e^{-i\phi_j} + \hat{A}_j^{\text{out}\dagger}(-\Omega)e^{i\phi_j}$ (which are not Hermitian and hence not observables), involve the two symmetric spectral components $\omega_j \pm \Omega$ for each field. We then introduce proper combinations of the signal and idler quadratures:

$$\hat{X}_-(t) = \frac{1}{\sqrt{2}}[\hat{X}_s(t) - \hat{X}_i(t-\Delta t)] \tag{14}$$

$$\hat{Y}_+(t) = \frac{1}{\sqrt{2}}[\hat{Y}_s(t) + \hat{Y}_i(t-\Delta t)], \tag{15}$$

where the delay Δt between the detection of the signal and idler arms can be used as an optimization parameter.

Next, we characterize the noise in the sum or difference modes by the so-called *squeezing spectra*:

$$\Sigma_\pm(\Omega) = \int d\tau e^{i\Omega\tau} \begin{cases} \langle \delta\hat{Y}_+(t)\delta\hat{Y}_+(t+\tau)\rangle, \\ \langle \delta\hat{X}_-(t)\delta\hat{X}_-(t+\tau)\rangle, \end{cases} \tag{16}$$

where, e.g., $\delta\hat{X}_- = \hat{X}_- - \langle\hat{X}_-\rangle = \hat{X}_-$ because below the threshold the field expectation values are zero. These quantities describe the degree of correlation ("−" sign) or anticorrelation ("+" sign) existing between the field quadrature operators of the twin beams at the two crystal output faces. The value "1" represents the shot-noise level, which corresponds to two uncorrelated light beams. In the degenerate case $\omega_s = \omega_i$, one may also think of physically recombining the two counterpropagating beams on a beam splitter, in order to produce two independently squeezed beams.

After some long but straightforward calculations, based on the input-output relations (4), one obtains

$$\Sigma_\pm(\Omega) = \tfrac{1}{2}\{|U_s(\Omega) - V_i^*(-\Omega)e^{i\Omega\Delta t}e^{i(\phi_s+\phi_i)}|^2 + |U_s(-\Omega) - V_i^*(\Omega)e^{-i\Omega\Delta t}e^{i(\phi_s+\phi_i)}|^2\}. \tag{17}$$

Up to this point we used only the Bogoliubov form of the relations (4), so that Eq. (17) actually holds for any PDC process. As expected for the EPR state, the degree of correlation and anticorrelation in orthogonal quadratures are identical: $\Sigma_-(\Omega) = \Sigma_+(\Omega)$. The two spectral terms on the right-hand side of Eq. (17) are present because detection of the temporal quadratures (12) probes the noise at $\omega_j \pm \Omega$ for each field. In the MOPO, these terms can be made identical by setting $\Delta t = \tau_{\text{gvm}}$, which exactly compensates the temporal offset of the twin beams. However, even in the absence of such optimization, the two terms are minimized by choosing

$$\phi_s + \phi_i = 2\theta(\pm\Omega) = \arg[U_s(\pm\Omega)V_i(\mp\Omega)] \tag{18}$$

$$\simeq k_s l_c + \phi_p + \arg[\text{sinc}\gamma(\Omega)] \pm \frac{\Omega}{\Omega_{\text{gvm}}} \tag{19}$$

$$\simeq k_s l_c + \phi_p + \arg[\text{sinc}\gamma(\Omega)], \tag{20}$$

where the second line uses the linear approximations (8) and (9) and the last line holds because $\Omega/\Omega_{\text{gvm}} \approx 0$ within the spectral region of interest. With this choice $\Sigma_\pm(\Omega) \to [|U_s(\Omega)| - |V_i(-\Omega)|]^2$ reaches its minimum value at any frequency, and the noise never goes above the shot-noise level "1". The degree of EPR correlation and anticorrelation $\Sigma_\mp(\Omega)$ is instead plotted in Fig. 2 for *fixed phase angles*, namely,

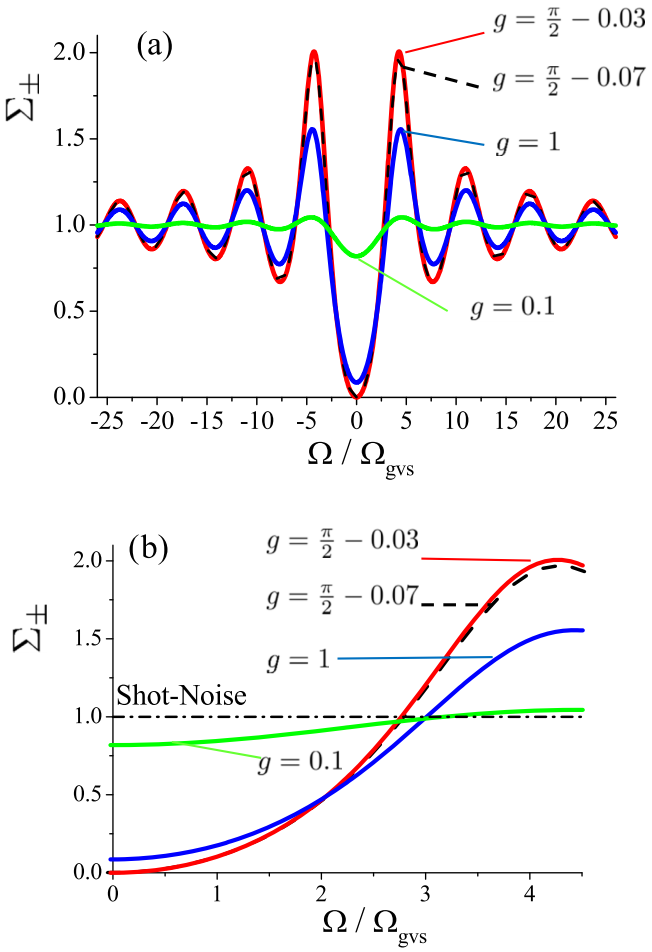

FIG. 2. Squeezing spectra $\Sigma_\pm(\Omega)$ (17), and degree of EPR correlation between the MOPO twin beams, as a function of $\Omega/\Omega_{\text{gvs}}$, for $\phi_s + \phi_i$ fixed as in Eq. (21). $\Delta t = 0$. (b) Detail of the minima.

$$\phi_s + \phi_i := 2\theta(0) = k_s l_c + \phi_p. \tag{21}$$

In this case, the noise passes from below to above the shot noise at $\Omega = \pm\Omega_{\text{gvs}}\sqrt{\pi^2 - g^2}$, where $\text{sinc}\gamma(\Omega)$ changes sign. These values can be used to define a bandwidth of squeezing $\Delta\Omega = \Omega_{\text{gvs}}\sqrt{\pi^2 - g^2} \approx 2.7\Omega_{\text{gvs}}$ close to threshold. Some remarks are in order. (i) The EPR correlation becomes asymptotically perfect as the MOPO threshold is approached, which can be realized only close to a critical point, because the noise in the quiet quadrature can be suppressed only at the expense of a diverging level of noise in the orthogonal one. (ii) The squeezing remains significant at rather large distances from threshold, $\Sigma_\pm(0) \simeq 0.09$ for $g = 1$, which is 36% below the MOPO threshold. (iii) Excellent levels of squeezing are present in the whole emission bandwidth, which we remind the reader is smaller than Ω_{gvs} [5]. This is in sharp contrast with the single-pass copropagating geometry, where high squeezing is difficult to observe [12] and the orientation of the squeezing ellipses varies rapidly inside the PDC bandwidth [17]. In contrast, for the MOPO the orientation of the ellipses, defined by $\theta(\pm\Omega)$, remains practically constant inside the bandwidth Ω_{gvs} [see Eqs. (18)–(20)]. This can be viewed as a consequence

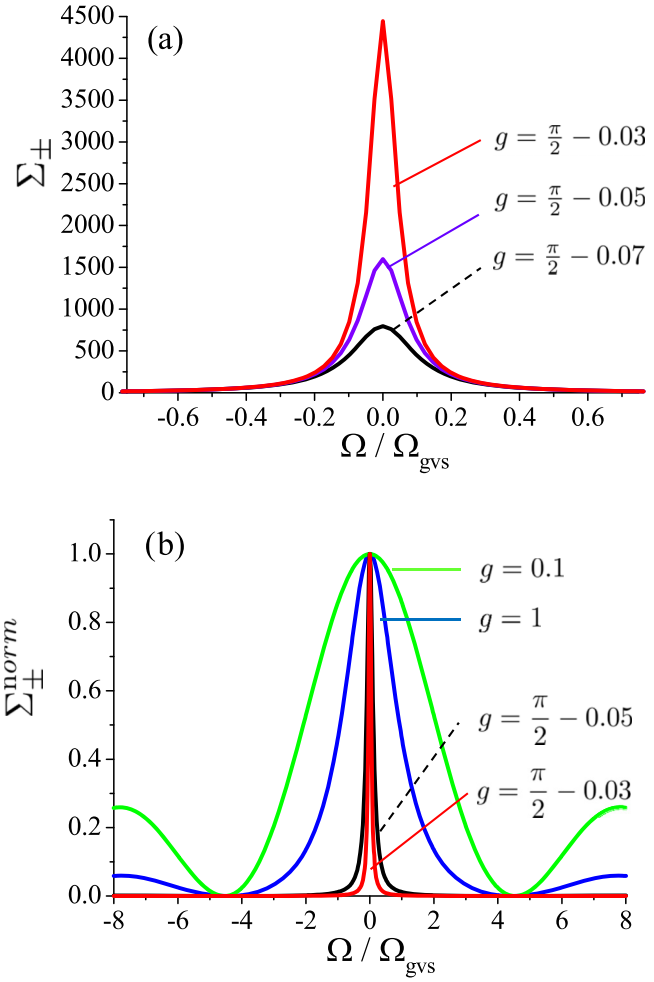

FIG. 3. Antisqueezing spectra $\Sigma_\pm(\Omega)$ (17) as a function of Ω/Ω_{gvs}, for phase angles orthogonal to those in Fig. 2. The curves in panel (b) are normalized inside $(0,1)$.

of the long (τ_{gvs}) and short (τ_{gvm}) time scales involved in the counterpropagating geometry.

Figure 3 shows the antisqueezing of the sum or difference modes, which occurs for quadrature phases orthogonal to those in Fig. 2. In this case the noise diverges upon approaching threshold, which is clearly reminiscent of the critical divergence of the MOPO spectra analyzed in Ref. [5]. The bandwidth of the antisqueezing spectra shrinks getting close to threshold [Fig. 3(b)], which again reflects the shrinking of the spectra and the critical slowing down of temporal fluctuations close to the MOPO threshold [5].

The curves in Figs. 2 and 3 are in a sense *universal* for the MOPO, when plotted as a function of $\frac{\Omega}{\Omega_{gvs}}$, and to a very good approximation hold for any material and tuning conditions. This can be more clearly seen by deriving explicit expressions of the noise spectra. By inserting the coefficients (5) into the general result (17), using the linear approximation (8) and neglecting the contribution of the slow phase $\beta(\Omega)$, when $\phi_s + \phi_i$ is fixed as in Eq. (21), the squeezing spectra can be written as

$$\Sigma_\pm^S(\Omega) = \frac{\sqrt{g^2+\tilde{\Omega}^2} - g\sin\sqrt{g^2+\tilde{\Omega}^2}}{\sqrt{g^2+\tilde{\Omega}^2} + g\sin\sqrt{g^2+\tilde{\Omega}^2}}, \tag{22}$$

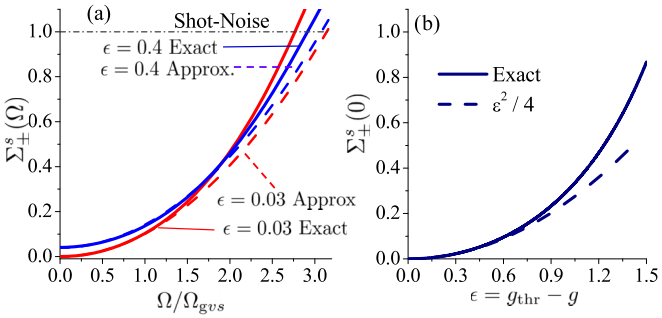

FIG. 4. Comparison between the exact results in Eq. (17) and the approximated ones in Eq. (23). Squeezing spectra (a) as a function of frequency and (b) at zero frequency as a function of the distance from threshold.

where $\tilde{\Omega} = \Omega/\Omega_{gvs}$. The antisqueezing spectra, for phases orthogonal to those in Eq. (21), are just the inverse, $\Sigma_\pm^A(\Omega) = 1/\Sigma_\pm^S(\Omega)$. This expressions take a particularly simple form in the neighborhood of threshold and for small frequencies. Let us define a distance from threshold, $\epsilon = g_{thr} - g$, and let us consider the limit $\epsilon \ll 1$ and $|\tilde{\Omega}| \ll g$. By expanding the various functions in Eq. (22) around $\epsilon = 0$ and $\tilde{\Omega}/g = 0$, and keeping terms at most quadratic in the small quantities, we obtain

$$\Sigma_\pm^S(\Omega) \underset{\substack{\epsilon\ll 1\\ |\tilde{\Omega}|\ll g}}{\longrightarrow} \frac{1}{4}\left(\epsilon^2 + \frac{\tilde{\Omega}^2}{g_{thr}^2}\right). \tag{23}$$

This function is a parabola which reaches its minimum at $\Sigma_\pm^S(0) = \frac{\epsilon^2}{4} \to 0$ as $\epsilon \to 0$, and of width $\Delta\tilde{\Omega} \approx 2g_{thr}$ constant close to threshold. In the same limit, the antisqueezing spectra become

$$\Sigma_\pm^A(\Omega) \underset{\substack{\epsilon\ll 1\\ |\tilde{\Omega}|\ll g}}{\longrightarrow} \frac{4}{\epsilon^2 + \frac{\tilde{\Omega}^2}{g_{thr}^2}}, \tag{24}$$

which represents a Lorentzian peak of diverging height $\frac{4}{\epsilon^2} \to \infty$ and of vanishing width $\Delta\tilde{\Omega} = \epsilon g_{thr} \to 0$, as threshold is approached. These approximated formulas nicely reproduce the minima and the maxima in Figs. 2 and 3, respectively, when not too far from threshold, and are actually valid for rather large distances from threshold, as shown by Fig. 4.

We notice that such behaviors of the squeezing spectra are completely comparable to what can be obtained in standard cavity OPOs below threshold (see, e.g., Ref. [18], formula (7.59), p. 131). Here, in the degenerate case, the spectrum of squeezing has the form

$$\Sigma^{OPO}(\Omega) = \frac{\left(A_p^{thr} - A_p\right)^2 + \bar{\Omega}^2}{\left(A_p^{thr} + A_p\right)^2 + \bar{\Omega}^2} \underset{|\bar{\Omega}|\ll 2}{\to} \frac{1}{4}(\epsilon^2 + \bar{\Omega}^2), \tag{25}$$

where A_p is a cavity gain parameter, proportional to the pump amplitude, the $\chi^{(2)}$ susceptibility, and the photon lifetime in the cavity; $\bar{\Omega}$ is the frequency normalized to the cavity linewidth; the OPO threshold is at $A_p = A_p^{thr} = 1$; and $\epsilon = A_p^{thr} - A_p$

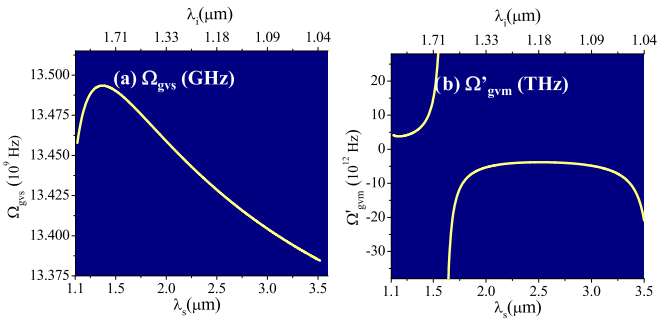

FIG. 5. Comparison between the two spectral scales of the MOPO for PPLN pumped at 800 nm, $l_c = 1$ cm. (a) $\Omega_{\rm gvs} = \frac{2}{l_c}(k'_s + k'_i)^{-1} \simeq$ 10 Ghz is the narrow MOPO bandwidth. (b) $\Omega_{\rm gvm} = \frac{2}{l_c}(k'_s - k'_i)^{-1}$ in the range 5 Thz or more is the broader GVM bandwidth. For each λ_s and λ_i the poling period is chosen to realize phase matching according to Eq. (1).

defines also in the OPO case the dimensionless distance from threshold. Remarkably, in both MOPO and OPO cases, the behavior $\sim\epsilon^2/4$ with the distance from threshold indicates that an excellent level of squeezing can be obtained even at rather large distances below the threshold.

As a final point, we remark that the spectra in Figs. 2 and 3 were calculated in the specific case of periodically poled lithium niobate (PPLN), pumped at 800 nm, with $\Lambda = 368$ nm, suitable to phase match the type 0 process at $\lambda_s = \lambda_i$ (Fig. 5). The wave numbers were evaluated using the complete Sellmeier relations in Ref. [19]. However, we did not notice appreciable differences (unless at very large frequencies of $\Omega \geqslant 15\Omega_{\rm gvs}$) in the linearly approximated results (22), nor in the curves obtained for different materials or tuning conditions, which confirms that our results are completely general for any MOPO configuration.

In conclusion, the MOPO below threshold is a source of EPR entangled beams over a wide range of light frequencies, including telecom wavelengths. Our analysis has shown that this cavityless configuration of PDC can reach the same narrowband, high level, and robust correlation characteristic of the cavity OPO, which represents the golden standard for EPR beams. As such, it can be used as an alternative to the OPO, meeting the increasing demand for monolithic devices in the field of integrated quantum optics.

[1] A. Christ, A. Eckstein, P. J. Mosley, and C. Silberhorn, Pure single photon generation by type-ipdc with backward-wave amplification, Opt. Express **17**, 3441 (2009).

[2] A. Gatti, T. Corti, and E. Brambilla, Temporal coherence and correlation of counterpropagating twin photons, Phys. Rev. A **92**, 053809 (2015).

[3] A. Gatti and E. Brambilla, Heralding pure single photons: A comparision between counter-propagating and co-propagating twin photons, arXiv:1706.01790 [quant-ph].

[4] C. Canalias and V. Pasiskevicius, Mirrorless optical parametric oscillator, Nat. Photon. **1**, 459 (2008).

[5] T. Corti, E. Brambilla, and A. Gatti, Critical behavior of coherence and correlation of counterpropagating twin beams, Phys. Rev. A **93**, 023837 (2016).

[6] A. Einstein, B. Podolsky, and N. Rosen, Can quantum-mechanical description of physical reality be considered complete? Phys. Rev. **47**, 777 (1935).

[7] M. D. Reid, Demonstration of the Einstein-Podolsky-Rosen paradox using nondegenerate parametric amplification, Phys. Rev. A **40**, 913 (1989).

[8] Z. Y. Ou, S. F. Pereira, H. J. Kimble, and K. C. Peng, Realization of the Einstein-Podolsky-Rosen Paradox for Continuous Variables, Phys. Rev. Lett. **68**, 3663 (1992).

[9] C. C. Gerry and P. L. Knight, *Introductory Quantum Optics* (Cambridge University Press, Cambridge, England, 2005), Chap. 7, pp. 167–169 and pp. 182–187.

[10] S. Lemieux, M. Manceau, P. R. Sharapova, O. V. Tikhonova, R. W. Boyd, G. Leuchs, and M. V. Chekhova, Engineering the Frequency Spectrum of Bright Squeezed Vacuum via Group Velocity Dispersion in an SU(1,1) Interferometer, Phys. Rev. Lett. **117**, 183601 (2016).

[11] A. L. Porta and R. E. Slusher, Squeezing limits at high parametric gains, Phys. Rev. A **44**, 2013 (1991).

[12] Y. Eto, T. Tajima, Y. Zhang, and T. Hirano, Observation of quadrature squeezing in a $\chi(2)$ nonlinear waveguide using a temporally shaped local oscillator pulse, Opt. Express **16**, 10650 (2008).

[13] F. Kaiser, B. Fedrici, A. Zavatta, V. D'Auria, and S. Tanzilli, A fully guided-wave squeezing experiment for fiber quantum networks, Optica **3**, 362 (2016).

[14] S. E. Harris, Proposed backward wave oscillation in the infrared, Appl. Phys. Lett. **9**, 114 (1966).

[15] T. Suhara and M. Ohno, Quantum theory analysis of counter-propagating twin photon generation by parametric downconversion, IEEE J. Quant. Electron. **46**, 1739 (2010).

[16] Y. J. Ding and J. B. Khurgin, Backward optical parametric oscillators and amplifiers, IEEE J. Quant. Electron. **32**, 1574 (1996).

[17] A. Gatti, T. Corti, and E. Brambilla, Quantum properties of backward parametric down-conversion (unpublished).

[18] D. F Walls and G. J. Milburn, *Quantum Optics* (Springer-Verlag, Berlin, 1994), Chap. 7, pp. 121–131.

[19] D. N. Nikogosian, *Nonlinear Optical Crystals: A Complete Survey* (Springer, New York, 2005).